# A Bienzymatic Biocatalyst Constituted by Glucose Oxidase and Horseradish Peroxidase Immobilized on Ordered Mesoporous Silica

*Federica Pitzalis, Maura Monduzzi, Andrea Salis**

Department of Chemical and Geological Sciences, University of Cagliari-CSGI and CNBS,

Cittadella Universitaria, S.S. 554 bivio Sestu, 09042- Monserrato (CA), Italy;

*CORRESPONDING AUTHOR FOOTNOTE. Tel.: +39070675 4362. Fax: +39 0706754388

Email: asalis@unica.it, monduzzi@unica.it

**Abstract**

It is presently extremely challenging to realize an active immobilized multi-enzyme biocatalyst which allows to run *in vitro* multi-step cascade reactions. This work deals with the obtainment of a bienzymatic immobilized biocatalyst constituted by Glucose Oxidase (GOx) and Horseradish Peroxidase (HRP) immobilized onto SBA-15 mesoporous silica. The effect of co-immobilization (GOx/HRP@SBA-15) versus the separated immobilization (GOx@SBA-15/HRP@SBA-15), and the effect of covalent versus physical immobilization, on protein loading and enzymatic activity were investigated. Regardless the different immobilization strategy used, it was found that the catalytic activity could be retained only if the immobilized bienzymatic biocatalyst was kept wet. The obtained wet GOx/HRP@SBA-15 biocatalyst could be recycled 14 times keeping a good activity. Finally, the bienzymatic biocatalyst was tested for the oxidation of two model phenolic (caffeic acid and ferulic acid) pollutants of agricultural wastewaters, as olive mill wastewaters (OMWs). The biocatalyst was able to reach a 70% conversion within 15 minutes.

**Keywords**: Bienzymatic biocatalyst, glucose oxidase, horseradish peroxidase, SBA-15 mesoporous silica, phenolic compounds.

## 1. Introduction

Ordered mesoporous silica (OMS) is a promising material for several technological applications because of its outstanding features [1]. Among the different possible applications, OMSs are being used in nanomedicine [2,3], adsorption [4], inorganic catalysis [5], and biocatalysis [6]. In particular, the use of OMSs as enzyme supports for immobilized biocatalysts seems to be a very feasible application, as demonstrated by the huge number of papers and recent reviews [6–9]. Among the enzymes immobilized on OMSs, which retained their activity after the immobilization, there are: chloroperoxidase [10], lipase [11,12], cytochrome c [13], xylanase [13], lysozyme [14], myoglobin [15], laccase [16], subtilisin [17], and many others [18]. The easiest method to carry out enzyme immobilization is physical adsorption. For physically adsorbed enzymes immobilization conditions, i.e. pH [15], ionic strength and electrolyte type have been shown to affect both enzyme loading and activity [19]. In general covalently bound enzymes are more stable to harsh reaction conditions and can be reused for several reaction cycles [20].

Most of previous works investigated the immobilization and the catalytic activity of only one enzyme immobilized on OMS. Very less common is the immobilization of two enzymes which work sequentially [21]. For example, Hartmann and coworkers were likely the first to immobilize glucose oxidase and chloroperoxidase on SBA-15 OMS to obtain a "tandem biocatalyst" [22]. The importance of that approach is due to the fact that chloroperoxidase is known to be susceptible to oxidative deactivation by hydrogen peroxide. *In situ* $H_2O_2$ formation through enzymatic glucose oxidation, carried out by glucose oxidase immobilized on SBA-15, was indeed found to avoid this problem.

Glucose oxidase (GOx; E.C.1.1.3.4 ) [23] and Horseradish peroxidase (HRP; E.C. 1.11.1.7) [24] are two versatile redox enzymes which are being used in biosensing [25,26], tissue engineering [27], and are very promising candidates for green chemistry [28] and bioremediation applications [29]. GOx oxidizes glucose to gluconolactone and reduces oxygen to $H_2O_2$, using

flavin adenin dinucleotide as the cofactor. HRP is a heme protein which uses $H_2O_2$ to oxidize various aromatic substrates. It has been shown that, similarly to chloroperoxidase, also HRP is a "suicide" enzyme, that is inactivated by high concentrations of its own substrate ($H_2O_2$) [22,30–33]. Hence, HRP activity could be retained by producing *in situ* a controlled amount of $H_2O_2$. This suggests the combined use of GOx and HRP for the realization of a bienzymatic biocatalyst.

GOx and HRP enzymes have been immobilized on several supports [21]. Most of those works were interested to the realization of a glucose biosensor [34,35]. But a novel and interesting application might be their use in bioremediation. For example, Phuoc et al. used GOx and HRP encapsulated onto phospholipids–templated silica, for the removal of polyciclyc aromatic hydrocarbons from wastewaters [29]. Another interesting application is the oxidation of recalcitrant phenolic compounds. These compounds are present in the aqueous effluents of some important agricultural processes like coffee [36] and olive oil production [37]. Phenolic compounds are highly pollutant substances which need to be removed before their release in the environment. Besides phenolic compounds, OMWs also contain carbohydrates, and glucose in particular [37]. This suggested us the possibility to use a GOx/HRP@OMS bienzymatic biocatalyst for the treatment of the recalcitrant phenolic compounds for bioremediation purposes in particular of OMWs which is a big issue in the Mediterranean area [16,37]. To the best of our knowledge, this application has not been proposed yet.

In the present work we wanted to reach the following two goals. First of all we investigated different strategies for the obtainment of an active bienzymatic biocatalyst constituted by GOx and HRP immobilized on SBA-15 OMS. To this purpose, SBA-15 was firstly synthesized and characterized through different physico-chemical techniques. According to what shown in Scheme 1, we investigated: i. the optimal enzymatic GOx:HRP mass ratio; ii. the catalytic activities of the co-immobilized (HRP/GOx@SBA-15) and of the singly immobilized (HRP@SBA-15 and GOx@SBA-15) enzymes; iii. the effect of the drying process on the

enzymatic activity. The reuse of the biocatalyst for several reaction cycles was also demonstrated. The second goal was to give a "proof of concept" that the obtained active bienzymatic biocatalyst could be used for the detoxification of agricultural wastewaters, such as OMWs, which contain both glucose and recalcitrant phenolic compounds. To this purpose a model wastewater containing glucose and either caffeic acid or ferulic acid was used a substrate solution for the bienzymatic biocatalyst. Caffeic acid and ferulic acid are two model recalcitrant phenolic compounds, common pollutants of olive mill and coffee production wastewaters [16,29,36].

## 2. **Materials and methods**

### **2.1 Chemicals**

Glucose oxidase (GOx) type VII from *Aspergillus niger* lyophilized (145 U $mg^{-1}$), Horseradish peroxidase (HRP) type I lyophilized salt free (250 U $mg^{-1}$), 2,2′-azinobis-(3-ethylbenzothiazoline-6-sulfonate) diammonium salt (ABTS, ≥98%), glutaraldehyde (50 wt% in $H_2O$), tetraethylorthosilicate (TEOS, 98%), pluronic copolymer P123, 3-aminopropyltrimethoxysilane (APTES, 97%), bovine serum albumin (BSA, 98%), Bradford reagent, sodium phosphate dibasic (ACS Grade, ≥99%), citric acid monohydrate (≥99%), ethanol (98%), were purchased from Sigma-Aldrich. Sodium phosphate monobasic monohydrate (≥99%) was purchased from J.T. Backer. Sodium citrate (ACS Grade ≥99%) was purchased from Aldrich. Glucose (ACS Grade ≥99%) was purchased from Carlo Erba. Ferulic acid ((*E*)-3-(4-hydroxy-3-methoxyphenyl)prop-2-enoic acid, >98.0%), caffeic acid ((*E*)-3-(3,4-dihydroxyphenyl)prop-2-enoic acid, >95.0%), were from Fluka (Milan, Italy). Milli-Q water (resistivity > 18.2 MΩ $cm^{-1}$ at 25 °C) was used for all buffer and enzymatic solutions. Phosphate buffer 0.1M pH 8, and 0.025M citrate buffer pH 5 were used for to prepare the enzymatic solutions for the immobilization process.

## 2.2 Synthesis and characterization of SBA-15 mesoporous silica

SBA-15 mesoporous silica was synthesized and functionalized with APTES according to the method described in previous works [20]. Small angle X-rays scattering (SAXS) patterns were recorded for 3600 s by means of a S3-MICRO SWAXS camera system (HECUS X-ray Systems, Graz, Austria). Cu-Kα radiation of wavelength 1.542 Å was provided by a GeniX X-rays generator, operating at 30 kV and 0.4 mA. A 1D-PSD-50M system (HECUS X-ray Systems, Graz, Austria) containing 1024 channels of width 54.0 μm was used for the detection of scattered X-rays in the small-angle region. Transmission electron microscopy (TEM) images were obtained on a JEOL 100S microscope. Finely ground samples were placed directly onto Formvar-coated electron microscopy nichel grids.

Textural analysis was carried out using an ASAP2020 (Micromeritics ), by determining the $N_2$ adsorption/desorption isotherms at 77 K. Before analysis, pure silica samples (SBA-15) were heated up to 250 °C at a rate of 1°C/min under vacuum, while the functionalized samples (SBA-15-$NH_2$, GOx/HRP@SBA-15) were outgassed overnight at 40°C. The specific surface area, and the pore size distribution were assessed by the Brunauer-Emmett-Teller (BET) and BJH methods, respectively.

Fourier Transform Infrared (FTIR) spectra were determined through a Bruker Tensor 27 spectrophotometer equipped with a diamond-ATR accessory and a DTGS detector. A number of 256 scans at a resolution of 2 $cm^{-1}$ were acquired in the range 4000–400 $cm^{-1}$.

## 2.3 Immobilization of GOx and HRP on SBA-15

*2.3.1 covalent co-immobilization.* The covalent co-immobilization of GOx and HRP on SBA-15, to obtain the GOx/HRP@SBA-15 biocatalyst, was carried out by putting in a 2 mL Eppendorf test tube 25 mg of amino functionalized SBA-15, 550 μL of 0.1 M phosphate buffer at pH 8, and 20 μL of glutaraldehyde solution (50 wt% in $H_2O$). The test tube was left under

stirring for 30 minutes until the white silica particles became red. Then the excess of glutaraldehyde was removed through extensive washing of the functionalized sample with fresh buffer. Two separated solutions of GOx and HRP both, at the concentration 2 mg/mL, were prepared by dissolving the enzymatic powders in 0.1 M phosphate buffer at pH 8. The GOx solution (2 mg/mL) and the HRP solution (2 mg/mL) were suitably mixed together to obtain different mass ratios (GOx:HRP = 1:1; 2:1; 3:1; 5:1 7:1). Then, 1 mL of the resulting bi-enzymatic solution was added to an Eppendorf test tube containing the glutaraldehyde-activated silica support, and left under stirring in a Eppendorf thermomixer at 25°C for 48h. The protein loading of the immobilized biocatalyst was determined according to what reported in the next paragraph. The bienzymatic biocatalyst was collected by centrifugation, washed three times, and dried overnight under vacuum at room temperature (dry biocatalyst). Alternatively, the samples were stored and then checked for activity without performing the drying step (wet biocatalyst).

*2.3.2 Separated covalent immobilization.* The separated immobilization of GOx and HRP on SBA-15, to obtain the GOx@SBA-15/HRP@SBA-15 biocatalyst, was carried out by putting in a 2 mL Eppendorf test tube 5 mg of amino functionalized SBA-15, 550 μL of 0.1 M phosphate buffer at pH 8, and 20 μL of glutaraldehyde (50 wt% in $H_2O$). Then 200 μL of either a HRP solution (2mg/mL in 0.1 M phosphate buffer at pH 8) or a GOx solution (2mg/mL in 0.1 M phosphate buffer at pH 8) were added. The samples were left under stirring for 48 h. The dispersion was then centrifuged and the obtained solid was washed twice with fresh buffer. The immobilized biocatalysts were both kept wet, and collected together to get 10 mg of immobilized bienzymatic biocatalyst to be used for the activity measurements.

*2.3.3 Physical immobilization of HRP.* The physical immobilization of HRP on SBA-15-$NH_2$ was carried out by adding to 5 mg of amino-functionalized support 200 μL of a 2 mg/mL HRP

solution in either citrate buffer (0.025 M; pH 5) or phosphate buffer (0.1 M; pH 8). The samples were left under stirring for 48 h. The dispersion was then centrifuged and the obtained solid was washed twice with fresh buffer. After the immobilization step the obtained biocatalyst was dried under vacuum or left wet according to what described above.

All samples were prepared at least in triplicate.

### 2.4 Determination of protein loading

The protein loading of the immobilized biocatalysts was determined by measuring the protein concentration of the immobilizing solution at fixed times. The protein concentration was obtained by means of a spectrophtometric calibration line (λ=595nm) prepared using a Bradford microassay. BSA solutions in 0.0125 M phosphate buffer at pH 8 in the concentration range 0.5-8 μg/mL were used to build the calibration curve.

Unless differently specified, protein loading, $q$ ($mg_{protein} \times g_{SBA\text{-}15}^{-1}$) was calculated according to the equation [38]:

$$q = \frac{([P]_0 - [P]_f)V - [P]_w V_w}{m_{SBA-15}} \qquad (1)$$

where, $[P]_0$ and $[P]_f$ are the protein concentration ($mg_{protein}/mL_{solution}$) at time t=0 and t=48h; V is the volume of the protein solution (mL), $m_{SBA\text{-}15}$ is the mass of SBA-15 (g).

The kinetics of loading process was investigated by measuring the protein concentration decrease at fixed times. Then different kinetic models were used to calculate the protein loading at equilibrium ($q_e$). According to a previous study [38], we fitted the kinetic data through the following equations:

$$q_t = \frac{q_e t}{a + t} \qquad (2)$$

where, $q_t$ is the protein loading at time $t$ .

Alternatively, kinetic data were analyzed by means of a pseudo-second order model [39]:

$$\frac{t}{q_t} = \frac{1}{k_2 q_e^2} + \frac{1}{q_e} t \quad (3)$$

Where $k_2$ is the pseudo-second order rate constant (h g $mg^{-1}$).

Finally, data were also analyzed through an 'intraparticle diffusion' model [39]:

$$q_t = x_i + k_i t^{1/2} \quad (4)$$

Where $k_i$ (mg $g^{-1}$ $h^{1/2}$) is the intraparticle diffusion constant, and $x_i$ is the intercept.

### 2.5 Activity assays

The enzymatic activities of the co-immobilized and singly immobilized biocatalysts were determined by UV/Vis spectrophotometry. A volume of 5600 μL of 25 mM citrate buffer pH5, 20-200 μL of glucose 0.5 M, and 20-200 μL of ABTS 0.02 M were added to 10 mg of immobilized bienzymatic biocatalyst. According to Scheme 2, GOx catalyzes the oxidation of glucose to gluconolactone which results in the *in situ* production of $H_2O_2$. The latter is used by HRP to oxidize ABTS. The formation of ABTS oxidized product as a function of time is followed by reading the absorbance at λ = 415 nm [40] (molar extinction coefficient, $\varepsilon_{ABTS}$ = $3.47\times10^4$ L $mol^{-1}$ $cm^{-1}$) [41]. Enzymatic activity is defined as the amount (μmoles) of ABTS transformed per minute ($\mu mol_{ABTS}$ $min^{-1}$). Specific activity defined as the enzymatic activity per mg of protein ($\mu mol_{ABTS}$ $min^{-1}$ $mg^{-1}$).

### 2.6 Stability of the immobilized bienzymatic biocatalyst.

In order to investigate the thermal stability of the GOx/HRP@SBA-15 biocatalyst, a sample of 10 mg was suspended in 500 μL of 100 mM phosphate buffer at pH 8 in an Eppendorf test tube and incubated in a Eppendorf thermomixer for 1 h at the selected temperature (25, 30, 35, 40 and 50°C). After that time, the sample was left to reach room temperature, and the liquid phase was removed after centrifugation. The enzymatic activity was then measured through the

spectrophometric assay described in the paragraph 2.5. Each experiment at different temperature was done at least in triplicate.

The storage stability of the GOx/HRP@SBA-15 wet biocatalyst was investigated by measuring the enzymatic activity after 10 days storage at 4°C by means of the activity assay described in paragraph 2.5. Experiments were done at least in triplicate.

Operational stability to recycling of the immobilized biocatalyst was studied by measuring the activity of the immobilized preparation according to what described in the paragraph 2.5 (1$^{st}$ cycle). Then the reaction suspension was centrifuged, the liquid phase removed and the assay repeated adding to the solid (biocatalyst) phase fresh buffer and substrates (see par. 2.5 for the quantities). This procedure was repeated 14 times.

### 2.7 Enzymatic removal of phenolic compounds

The enzymatic removal of the phenolic compounds, ferulic acid (FAc) and caffeic acid (CAc), was carried out by adding to 10 mg of immobilized bienzymatic biocatalyst 5 mL of a solution containing 1 mL of the phenolic compound at 5 mg/mL and 4 mL of glucose 0.5M at 298 K. The disappearance of the phenolic compounds was quantified spectrophometrically by means of suitable calibration curves obtained at $\lambda$ = 286 nm and $\lambda$ = 310 nm for FAc and CAc respectively.

## 3. Results and discussion

### 3.1 synthesis and Characterization of Mesoporous SBA-15

SBA-15 mesoporous silica was firstly synthesized and characterized before to be used as a support for enzyme immobilization. Fig. 1 shows the structural characterization carried out through transmission electron microscopy (TEM, Fig.1A) and small angle X-rays scattering (SAXS, Fig. 1B). Both techniques confirm that the synthesized sample has an ordered structure with an hexagonal array of parallel channels. Moreover, SAXS analysis permits to measure the

lattice parameter *a* = 11.7 nm. The textural characterization was then carried out by determining $N_2$ adsorption/desorption isotherms. The physisorption curve (Fig. 1C) shows a type IV isotherm with a H1 hysteresis loop, typical of mesoporous materials with parallel channels. From the adsorption data a surface area of 880 $m^2 g^{-1}$, and a pore volume of 1.25 $cm^3 g^{-1}$ were estimated. A monomodal pore size distribution with a maximum at 6.7 nm (Fig. 1D) was calculated through the BJH model. Table 1 summarizes the textural and structural data of SBA-15. The SBA-15 sample was functionalized with aminopropyltriethoxysilane to obtain the amino functionalized SBA-15-$NH_2$ sample. This was needed for the covalent immobilization of the enzymes as described in the next paragraphs. The functionalization procedure does not change the structure as confirmed by SAXS (Fig. 1B) but affects the textural properties. Indeed, the surface area became 373 $m^2 g^{-1}$, pore volume 0.65 $cm^3 g^{-1}$, and pore size 5.5 nm (Table 1). A possible reason of the observed change of surface area and pore volume due to APTES functionalization is likely the filling of SBA-15 microporous volume. Indeed, if we look at the initial part (low p/p0 values) of the adsorption isotherm (Figure 1C), we see a much lower volume of gas adsorbed for SBA-15-$NH_2$ with respect to SBA-15. However, these changes are consistent with what described in previous works [42–44]

ATR-FTIR spectroscopy was used for a further analysis (Fig.1E). The spectrum shows the characteristic IR absorption bands for Si-O-Si asymmetric and symmetric stretching vibration at the wavenumbers of 1070 $cm^{-1}$ and 800 $cm^{-1}$ respectively. One intense band nearby 450 $cm^{-1}$ is due to Si-O-Si bending. The broad band around 3300 $cm^{-1}$ is due to the O-H stretching of adsorbed water. The functionalization with APTES causes the disappearance of the peak at 980 $cm^{-1}$, due to Si-OH vibration, whereas a weak peak at 1554 $cm^{-1}$ (Fig. 1F) is attributed to the asymmetric bending of -$NH_2$ groups in SBA-15-$NH_2$, and a weak band around 2940 $cm^{-1}$ is due to the stretching of C-H bond of the aminopropyl group (Fig. 1F).

### 3.2 Covalent co-immobilization of GOx and HRP on SBA-15 mesoporous silica

*3.2.1 Characterization of GOx/HRP@SBA-15 immobilized biocatalyst.*

The covalent co-immobilization GOx and HRP on amino functionalized SBA-15, using glutharaldheyde as the chemical linker, was firstly investigated. The obtained sample was characterized through SAXS, $N_2$ adsorption/desorption isotherms, and FTIR spectroscopy. The obtained results are the green curves shown in Fig. 1B-E. We observe in Fig. 1B that the structure of SBA-15-$NH_2$ is not affected by the enzyme immobilization process, as also confirmed by the same value of the lattice parameter, $a$ = 11.9 nm, (Table 1). Textural characterization (Fig. 1C-D) instead, gave a surface area of 166 $m^2\ g^{-1}$, a pore volume of 0.24 $cm^3\ g^{-1}$, and a pore size of 3.6 nm. The reduction of these textural parameters, respect to the values of SBA-15-$NH_2$ sample, is consistent with enzyme immobilization within the pores of mesoporous silica (Table 1). FTIR analysis (Fig. 1F) confirms the successful enzyme immobilization due to the occurrence of the two peculiar peaks, amide I and amide II, at 1650 $cm^{-1}$ and 1550 $cm^{-1}$ respectively [45].

*3.2.2 Immobilization kinetics.*

We then investigated the immobilization kinetics focusing on the effect of different GOx:HRP mass ratios. This was done because a different enzyme mass ratio should result in a different instantaneous concentration of $H_2O_2$ available for ABTS oxidation. As shown in the next paragraph, this can either favor or disfavor the biocatalyst's performance.

Fig. 2 shows the effect of different GOx:HRP mass ratios on the adsorption kinetics. In particular Fig. 2A displays the increase of enzyme loading as a function of time. The protein concentration sharply decreased at initial times ($t < 10$ h), then reached the equilibrium after about 24 h. Longer times gave only a small loading increase (Fig. 2A). Among the used kinetic models - that is, the pseudo-second order (eq. 3; Fig. 2B) and the intraparticle diffusion model (eq. 4; Fig 2C) - the latter is of particular interest since it can provide useful information about the mechanism of the adsorption process. In general, enzyme immobilization occurs through a

multi-step mechanism. The plot of the intraparticle diffusion model reports $q_t$ (protein loading at time t) in the y axis versus $t^{1/2}$ in the x axis. Generally the data can be fitted through 2 or 3 straight lines having different slopes. Each slope is associated to one of the steps of the immobilization mechanism. The data shown in Fig 2C are indeed consistent with a two step process. Table 2 lists the values of protein loading at equilibrium ($q_e$) obtained for the immobilization experiments. The $q_e$ values, expressed as $mg_{protein} \times g_{SBA\text{-}15}^{-1}$, range between 30-40 mg $g^{-1}$ for most GOx:HRP mass ratios. The loading values obtained through fitting procedures (using eq.s 2 and 3), were consistent with those obtained by subtracting the protein amount at the times t = 0 h and t = 48 h (eq. 1).

### 3.3 Catalytic activity of the immobilized biocatalyst

*3.3.1 Co-immobilized GOx/HRP@SBA-15*

The different co-immobilized enzyme (dried) samples having different GOx:HRP ratios (2:1; 1:1; 1:2; and 1:3) were checked for enzymatic activity. Results in Fig. 3 show that for GOx/HRP@SBA-15 biocatalyst, the ratio GOx:HRP = 1:1 has the highest activity among those tested. Nevertheless, we noticed that the measured activity was very low if compared to that of the free enzymes, which was 26.1 $\mu mol_{ABTS} \times min^{-1}$ for the mass ratio GOx:HRP = 1:1 (data not shown). An activity loss due to the immobilization process is not a strange result since already observed in previous works [12]. Nevertheless, in order to understand the possible causes of such a low activity some qualitative experiments were carried out. The addition of suitable volumes of aqueous free GOx and free HRP solutions to two different test tubes containing the immobilized biocatalyst suspended in the substrate (glucose and ABTS) solution gave very interesting qualitative results. Indeed, the test tube containing the free GOx and the co-immobilized biocatalyst was inactive, whereas that containing the free HRP and the co-immobilized biocatalyst was highly active. This observation suggests that the immobilized HRP is inactive, whereas the immobilized GOx is still active.

*3.3.2 Comparison between the separately immobilized GOx@SBA-15/HRP@SBA-15 and coimmobilized GOx/HRP@SBA-15 biocatalysts.*

In order to try to increase the low biocatalyst activity we tried different immobilization strategies and compared the corresponding catalytic activities. More in detail, the covalent immobilization of GOx and HRP on SBA-15 was carried out separately to obtain GOx@SBA-15 and HRP@SBA-15 biocatalysts. In this experiment the immobilized biocatalysts were both dried under vacuum, and then mixed together after the immobilization. The activity was measured by adding a solution containing the mixture of glucose and ABTS substrates. Also for the separately immobilized enzymes, GOx@SBA-15/HRP@SBA-15 (Table 3), the specific activity was 0.4±0.1 μmol $min^{-1}$ $mg^{-1}$ that is even lower than that measured for the co-immobilized biocatalyst GOx/HRP@SBA-15 (1.6±0.3 μmol $min^{-1}$ $mg^{-1}$, Table 3). From previous and present results we found that the loss of activity is mainly imputable to the immobilized HRP. Indeed, HRP seems to be more sensitive to the covalent immobilization process than GOx which keeps its activity at a higher extent after immobilization both in the singly and in the co-immobilized biocatalysts. Although the covalent immobilization generally results in a more stable biocatalyst, it can result into the distortion of the enzyme structure which may lead to a partial or full inactivation. Then, in order to determine if the covalent binding to SBA-15 was critical for HRP, its physical adsorption at two different pH values (5 and 8) was carried out. Although the loading of HRP can be modulated by a change of pH in the physical immobilization process, the activity is again very low and comparable to that of the covalent immobilized GOx@SBA-15/HRP@SBA-15 biocatalyst (Table 3). Hence, the use of the separately immobilized bienzymatic biocatalyst does not give any advantage in terms of activity, regardless HRP is covalently or physically immobilized. The results above have demonstrated that the activity of the bienzymatic biocatalyst does not depend on the fact that the enzymes are co-immobilized or singly immobilized on SBA-15 mesoporous silica. Moreover,

not even the type of immobilization (covalent versus physical) is responsible for the low activity of the biocatalyst.

*3.3.3 Activity of dry versus wet biocatalyst*

Another possible reason for the low biocatalyst activity might be due to the water content of the immobilized preparation. For free enzymes it is well known that enzymes are better stored in solid rather than in liquid form [46]. In order to obtain a solid preparation, water needs to be removed for example through freeze-drying. This and similar processes are seen to result in a partial or total loss of enzyme activity which can be limited by the addition of stabilizers (i.e. carbohydrates) [46]. For immobilized enzymes, it is a common procedure to dry, usually under vacuum at room temperature, the obtained wet biocatalyst. This because a dried preparation can be weighed, manipulated, and stored more easily than a wet one. Similarly, to the case of free enzymes, it may happen that the drying process can result in the partial or full enzyme inactivation. In the literature there are contrasting information about this issue for GOx and HRP enzymes. Dai et al. prepared a modified glassy carbon electrode by dropping upon it a GOx-HRP/SBA-15 suspension. This modified electrode was used after drying for 3h in ambient conditions [34]. Yang et al. instead stored the immobilized bienzymatic system suspended in suitable buffer solutions [47]. Similarly [48], stored the enzymes in aqueous solution at pH 7 and 4°C. Cao et al. stored the biocatalyst at 4°C without specifying if it had been dried or not [35]. Hence, it is of fundamental importance to understand if the drying process is critical for the activity of GOx and HRP. For these reasons we measured the activity of the bienzymatic biocatalyst where GOx@SBA-15 was, as usual, dried under vacuum while HRP@SBA-15 was kept wet. The specific activity of the singly immobilized GOx@SBA-15/HRP@SBA-15 bienzymatic biocatalyst was 18±8 μmol $min^{-1}$ $mg^{-1}$, that is about one order of magnitude higher than the bienzymatic biocatalyst where HRP@SBA-15 was dried (Table 3). Even more interesting is the fact that the activity of the wet co-immobilized biocatalyst was about two order

of magnitude higher (116±27 μmol $min^{-1}$ $mg^{-1}$) than that of the same type of dried biocatalyst. This means that although GOx is less sensitive to drying than HRP it has, anyway, a substantial benefit to remain hydrated instead of being dried.

### 3.4 Stability of the immobilized bienzymatic biocatalyst

#### *3.4.1 Thermal and storage stability*

Once ascertained that the immobilized bienzymatic biocatalyst is active only if kept wet, it is important to check its thermal, storage and operational stability. Fig. 4A shows the specific activity of the immobilized GOx/HRP@SBA-15 biocatalyst after 1 hour incubation at different temperatures in the range 25°C - 50°C. The immobilized biocatalyst has a slight increase in activity at 30°C, but already at 35°C we observe a sudden activity decrease. Finally, the incubation at 50°C results in a quasi full inactivation of the immobilized biocatalyst. Fig. 4B, instead shows, the storage stability of the immobilized biocatalyst. GOx/HRP@SBA-15 was stored for 10 days at 4°C. The effect of storage was to decrease the specific activity of the immobilized bienzymatic biocatalyst from the initial value of 116±27 μmol $min^{-1}$ $mg^{-1}$ to about 45±9 μmol $min^{-1}$ $mg^{-1}$. Previous findings suggest that this low thermal and storage stability of the bienzymatic biocatalyst is likely imputable to HRP [49] rather than the more robust GOx enzyme.

#### *3.4.2 Operational stability: Biocatalyst recycling*

One of the main goals of immobilized enzymes is the possibility of their reuse. This because enzymes are generally very expensive respect to traditional chemical catalysts. Besides their high cost, enzymes are also highly unstable in their native, and active, conformation. For these reasons, enzyme immobilization permits to recover the biocatalyst particles (i.e. by filtration or centrifugation), and also to stabilize the enzyme in its active conformation. In addition, here we

have seen that the hydration of the immobilized biocatalyst plays an important role to determine the activity. Fig. 5 displays the reuse of the immobilized biocatalyst for different reaction cycles. In particular, we compared the dry singly immobilized bienzymatic biocatalyst GOx@SBA-15/HRP@SBA-15 (dry/dry) with that where the immobilized HRP was kept wet (dry/wet), and the wet co-immobilized GOx/HRP@SBA-15 biocatalyst. The dry separately immobilized biocatalyst had a very low specific activity and became fully inactive at the $7^{th}$ reaction cycle. The separately immobilized biocatalyst, where HRP@SBA-15 was kept wet, had a higher activity that was lost after the $6^{th}$ reaction cycle. Finally the wet co-immobilized biocatalyst was very active and could be reused several times, keeping a specific activity of about 60 μmol $min^{-1}$ $mg^{-1}$ at the $14^{th}$ reaction cycle. Hence, although the bienzymatic biocatalyst was not very stable to the thermal treatment and storage, its possible reuse for more than 14 reaction cycles is a remarkable result.

### 3.5 Enzymatic oxidation of recalcitrant phenolic compounds

A possible application of a bienzymatic biocatalyst could be the oxidation of water pollutants. For example [29] reported the oxidation of polycyclic aromatic hydrocarbons through an immobilized GOx/Hb (Hemoglobin) bienzymatic biocatalyst. Here, in order to test a potential application of the bienzymatic biocatalyst, we investigated the enzymatic oxidation of two phenolic compounds contained in OMWs. OMWs have a complicated composition in phenolic compounds, carbohydrates, organic acids and minerals [37]. Although OMWs are rich in nutrients, their release in the environment is not possible due to the phytotoxic action of phenolic compounds. Hence, a way to overcome this problem is to firstly oxidize phenolic compounds contained in OMWs. A similar problem occurs in those geographical areas, i.e. Brasil, where coffee is produced. Torres et al. studied the enzymatic oxidation of caffeic acid, a recalcitrant phenolic pollutant, contained in wastewaters of coffee production [36]. They compared the action of peroxidases of different sources by adding different amounts of $H_2O_2$.

As explained above a locally produced $H_2O_2$ is a key issue for "suicide" enzymes as peroxidases [30]. For this reason the sequential action of GOx and HRP in an immobilized bienzymatic biocatalyst seems to be a good option. Moreover, OMWs already contain carbohydrates and glucose in particular (from 4.8 % to 13.4 %) [37], thus there is no need to add external $H_2O_2$ as HRP substrate.

As a proof of concept of the possibility to use the bienzymatic biocatalyst for the degradation of phenolic compounds contained in OMWs we prepared two solutions containing glucose and either ferulic acid (FAc) or caffeic acid (CAc) . The disappearance of the phenolic compounds was investigated spectrophotometrically at the wavelength of 286 nm (FAc) and 310 nm (CAc). Fig. 6A shows the decrease of ferulic and caffeic acid concentration due to the action of the immobilized bienzymatic biocatalyst. Fig 6B shows that the two phenolic compounds reached a conversion of about 70% within 15 minutes. This result is better than what obtained by Torres et al. that at maximum reached 51% conversion of caffeic acid within 15 minutes [36] by means of peroxidase and external addition of $H_2O_2$. Thus, although the reaction did not reach completeness, it is nevertheless fast. Hence, the GOx/HRP@SBA-15 bienzymatic biocatalyst has a potential interest for environmental applications.

## 4. Conclusions

The present work investigated the realization of a bienzymatic biocatalyst constituted by GOx and HRP immobilized onto SBA-15 ordered mesoporous silica. Some important points about the activity of the obtained biocatalyst should be remarked. The activity of the bienzymatic biocatalyst does not depend on the fact that the system is constituted by a mixture of two singly immobilized enzymes, GOx@SBA-15/HRP@SBA-15, or by co-immobilized enzymes GOx/HRP@SBA-15. In fact, it is rather the drying process that constitutes the most critical issue. Indeed, although from one hand the drying permits an easy handling of the biocatalyst, on the other hand, it leads to the loss of most the enzymatic activity. In particular, the drying

process inactivates HRP at a higher extent than GOx. We also found that HRP is active when kept wet. This independently HRP is covalently or physically immobilized on SBA-15. The wet bienzymatic co-immobilized biocatalyst retained its activity for 14 reaction cycles. Finally, a possible application of the biocatalyst for bioremediation of OMWs was proposed. OMWs are highly pollutant by-product of olive oil production mainly based in the Mediterranean region. The phytotoxic nature of OMWs is due to the presence of recalcitrant phenolic compounds. But in the complex composition of OMWs also glucose occurs [37]. This suggested us the use of a GOx/HRP bienzymatic biocatalyst for the oxidation of phenolic compounds contained in OMWs. Hence, we modelled the biocatalytic treatment of OMWs by using a solution containing glucose and a phenolic compound, i.e. either caffeic or ferulic acid. The hydrogen peroxide produced by GOx-catalyzed glucose oxidation was used by HRP to oxidize ferulic acid and caffeic acid. The immobilized bienzymatic biocatalyst GOx/HRP@SBA-15 allowed to reach a conversion of about 70 mol% of the two phenolic compounds within only 15 min. To the best of our knowledge the use of a GOx/HRP bienzymatic system for the treatment of OMWs has not been proposed yet.These encouraging results require, nonetheless, a deeper investigation using more complex phenolic solutions and, ultimately, a test with a real OMWs sample.

## Acknowledgements

CSGI and CNBS are thanked for financial support. F.P. thanks Agenzia delle Dogane e dei Monopoli for financing her PhD scholarship. Prof. E. Sanjust is thanked for useful discussion and valuable advices.

## References

[1] B. Lebeau, A. Galarneau, M. Linden, Introduction for 20 years of research on ordered mesoporous materials., Chem. Soc. Rev. 42 (2013) 3661–3662. doi:10.1039/c3cs90005c.

[2] V. Mamaeva, C. Sahlgren, M. Lindén, Mesoporous silica nanoparticles in medicine-recent advances., Adv. Drug Deliv. Rev. 65 (2013) 689–702. doi:10.1016/j.addr.2012.07.018.

[3] M. Monduzzi, S. Lampis, S. Murgia, A. Salis, From self-assembly fundamental knowledge to nanomedicine developments., Adv. Colloid Interface Sci. 205 (2014) 48–67. doi:10.1016/j.cis.2013.10.009.

[4] Z.X. Wu, D.Y. Zhao, Ordered mesoporous materials as adsorbents, Chem. Commun. 47 (2011) 3332–3338. doi:Doi 10.1039/C0cc04909c.

[5] E.M. Usai, M.F. Sini, D. Meloni, V. Solinas, A. Salis, Sulfonic acid-functionalized mesoporous silicas: Microcalorimetric characterization and catalytic performance toward biodiesel synthesis, Microporous Mesoporous Mater. 179 (2013) 54–62. doi:10.1016/j.micromeso.2013.05.008.

[6] J.M. Bolivar, I. Eisl, B. Nidetzky, Advanced characterization of immobilized enzymes as heterogeneous biocatalysts, Catal. Today. 259 (2015) 66–80. doi:10.1016/j.cattod.2015.05.004.

[7] M. Hartmann, X. Kostrov, Immobilization of enzymes on porous silicas--benefits and challenges., Chem. Soc. Rev. 42 (2013) 6277–6289. doi:10.1039/c3cs60021a.

[8] N. Carlsson, H. Gustafsson, C. Thörn, L. Olsson, K. Holmberg, B. Åkerman, Enzymes immobilized in mesoporous silica: A physical–chemical perspective, Adv. Colloid Interface Sci. 205 (2014) 339–360. doi:10.1016/j.cis.2013.08.010.

[9] E. Magner, Immobilisation of enzymes on mesoporous silicate materials., Chem. Soc. Rev. 42 (2013) 6213–22. doi:10.1039/c2cs35450k.

[10] Y.J. Han, J.T. Watson, G.D. Stucky, A. Butler, Catalytic activity of mesoporous silicate-immobilized chloroperoxidase, J. Mol. Catal. - B Enzym. 17 (2002) 1–8. doi:10.1016/S1381-1177(01)00072-8.

[11] H. Gustafsson, E.M. Johansson, A. Barrabino, M. Odén, K. Holmberg, Immobilization of lipase from Mucor miehei and Rhizopus oryzae into mesoporous silica - the effect of varied

particle size and morphology, Colloids Surf. B. Biointerfaces. 100 (2012) 22–30. doi:10.1016/j.colsurfb.2012.04.042.

[12] A. Salis, D. Meloni, S. Ligas, M.F. Casula, M. Monduzzi, V. Solinas, et al., Physical and chemical adsorption of Mucor javanicus lipase on SBA-15 mesoporous silica. Synthesis, structural characterization, and activity performance, Langmuir. 21 (2005) 5511–5516. doi:10.1021/la047225y.

[13] S. Hudson, E. Magner, J. Cooney, B.K. Hodnett, Methodology for the immobilization of enzymes onto mesoporous materials, J. Phys. Chem. B. 109 (2005) 19496–19506.

[14] A. Vinu, V. Murugesan, M. Hartmann, Adsorption of Lysozyme over Mesoporous Molecular Sieves MCM-41 and SBA-15: Influence of pH and Aluminum Incorporation, J. Phys. Chem. B. 108 (2004) 7323–7330. doi:10.1021/jp037303a.

[15] H. Essa, E. Magner, J. Cooney, B.K. Hodnett, Influence of pH and ionic strength on the adsorption, leaching and activity of myoglobin immobilized onto ordered mesoporous silicates, J. Mol. Catal. B Enzym. 49 (2007) 61–68. doi:10.1016/j.molcatb.2007.07.005.

[16] A. Salis, M. Pisano, M. Monduzzi, V. Solinas, E. Sanjust, Laccase from Pleurotus sajor-caju on functionalised SBA-15 mesoporous silica: Immobilisation and use for the oxidation of phenolic compounds, J. Mol. Catal. B Enzym. 58 (2009) 175–180. doi:10.1016/j.molcatb.2008.12.008.

[17] K. Murai, T. Nonoyama, T. Saito, K. Kato, Enzyme structure and catalytic properties affected by the surface functional groups of mesoporous silica, Catal. Sci. Technol. 2 (2012) 310–315. doi:10.1039/c1cy00258a.

[18] Z. Zhou, M. Hartmann, Progress in enzyme immobilization in ordered mesoporous materials and related applications, Chem. Soc. Rev. 42 (2013) 3894–3912. doi:10.1039/c3cs60059a.

[19] A. Salis, L. Medda, F. Cugia, M. Monduzzi, Effect of electrolytes on proteins physisorption on ordered mesoporous silica materials, Colloids Surf. B. Biointerfaces. 137 (2016) 77–90. doi:10.1016/j.colsurfb.2015.04.068.

[20] A. Salis, M.F. Casula, M.S. Bhattacharyya, M. Pinna, V. Solinas, M. Monduzzi, Physical and Chemical Lipase Adsorption on SBA-15: Effect of Different Interactions on Enzyme Loading and Catalytic Performance, ChemCatChem. 2 (2010) 322–329. doi:10.1002/cctc.200900288.

[21] F. Jia, B. Narasimhan, S. Mallapragada, Materials-based strategies for multi-enzyme immobilization and co-localization: A review, Biotechnol. Bioeng. 111 (2014) 209–222. doi:10.1002/bit.25136.

[22] D. Jung, C. Streb, M. Hartmann, Oxidation of indole using chloroperoxidase and glucose oxidase immobilized on SBA-15 as tandem biocatalyst, Microporous Mesoporous Mater. 113 (2008) 523–529. doi:10.1016/j.micromeso.2007.12.009.

[23] H.J. Hecht, D. Schomburg, H. Kalisz, R.D. Schmid, The 3D structure of glucose oxidase from Aspergillus niger. Implications for the use of GOD as a biosensor enzyme, Biosens. Bioelectron. 8 (1993) 197–203. doi:10.1016/0956-5663(93)85033-K.

[24] N.C. Veitch, Horseradish peroxidase: A modern view of a classic enzyme, Phytochemistry. 65 (2004) 249–259. doi:10.1016/j.phytochem.2003.10.022.

[25] X. Yu, W. Lian, J. Zhang, H. Liu, Multi-input and -output logic circuits based on bioelectrocatalysis with horseradish peroxidase and glucose oxidase immobilized in multi-responsive copolymer films on electrodes, Biosens. Bioelectron. 80 (2016) 631–639. doi:10.1016/j.bios.2016.02.010.

[26] M. Mathew, N. Sandhyarani, Detection of glucose using immobilized bienzyme on cyclic bisureas-gold nanoparticle conjugate, Anal. Biochem. 459 (2014) 31–38. doi:10.1016/j.ab.2014.05.003.

[27] Q. Wei, M. Xu, C. Liao, Q. Wu, M. Liu, Y. Zhang, et al., Printable hybrid hydrogel by dual enzymatic polymerization with superactivity, Chem. Sci. 7 (2016) 2748–2752. doi:10.1039/C5SC02234G.

[28] A. Ramanavicius, A. Kausaite-Minkstimiene, I. Morkvenaite-Vilkonciene, P. Genys, R.

Mikhailova, T. Semashko, et al., Biofuel cell based on glucose oxidase from Penicillium funiculosum 46.1 and horseradish peroxidase, Chem. Eng. J. 264 (2015) 165–173. doi:10.1016/j.cej.2014.11.011.

[29] L.T. Phuoc, P. Laveille, F. Chamouleau, G. Renard, J. Drone, B. Coq, et al., Bridging the gap in catalysis via multidisciplinary approaches Guest, Dalt. Trans. 39 (2010) 8511–8520. doi:10.1039/C001146K.

[30] J. Rocha-Martin, S. Velasco-Lozano, J.M. Guisán, F. López-Gallego, Oxidation of phenolic compounds catalyzed by immobilized multi-enzyme systems with integrated hydrogen peroxide production, Green Chem. 16 (2014) 303. doi:10.1039/c3gc41456f.

[31] K.J. Baynton, J.K. Bewtra, N. Biswas, K.E. Taylor, Inactivation of horseradish peroxidase by phenol and hydrogen peroxide: A kinetic investigation, Biochim. Biophys. Acta - Protein Struct. Mol. Enzymol. 1206 (1994) 272–278. doi:10.1016/0167-4838(94)90218-6.

[32] J. a Nice, H. Wright, A model of peroxidase activity with inhibition by hydrogen peroxide, Enzyme Microb. Technol. 229 (1997) 302–310.

[33] K. Chattopadhyay, S. Mazumdar, Structural and conformational stability of horseradish peroxidase: effect of temperature and pH., Biochemistry. 39 (2000) 263–270. doi:10.1021/bi990729o.

[34] Z. Dai, J. Bao, X. Yang, H. Ju, A bienzyme channeling glucose sensor with a wide concentration range based on co-entrapment of enzymes in SBA-15 mesopores, Biosens. Bioelectron. 23 (2008) 1070–1076. doi:10.1016/j.bios.2007.10.015.

[35] X. Cao, Y. Li, Z. Zhang, J. Yu, J. Qian, S. Liu, Catalytic activity and stability of glucose oxidase / horseradish peroxidase co-confined in macroporous silica foam, Analyst. 137 (2012) 5785–5791. doi:10.1039/c2an36237f.

[36] J.A. Torres, P.M.B. Chagas, M.C. Silva, C.D. Dos Santos, A.D. Corrêa, Enzymatic oxidation of phenolic compounds in coffee processing wastewater, Water Sci. Technol. 73 (2016) 39–50. doi:10.2166/wst.2015.332.

[37] S. Dermeche, M. Nadour, C. Larroche, F. Moulti-Mati, P. Michaud, Olive mill wastes: Biochemical characterizations and valorization strategies, Process Biochem. 48 (2013) 1532–1552. doi:10.1016/j.procbio.2013.07.010.

[38] D. Steri, M. Monduzzi, A. Salis, Ionic strength affects lysozyme adsorption and release from SBA-15 mesoporous silica, Microporous Mesoporous Mater. 170 (2013) 164–172. doi:10.1016/j.micromeso.2012.12.002.

[39] T.P.B. Nguyen, J.W. Lee, W.G. Shim, H. Moon, Synthesis of functionalized SBA-15 with ordered large pore size and its adsorption properties of BSA, Microporous Mesoporous Mater. 110 (2008) 560–569. doi:10.1016/j.micromeso.2007.06.054.

[40] Y. Lee, J. Yoon, U. Von Gunten, Spectrophotometric determination of ferrate (Fe(VI)) in water by ABTS, Water Res. 39 (2005) 1946–1953. doi:10.1016/j.watres.2005.03.005.

[41] S. Scott, W. Chen, A. Bakac, J.H. Espenson, Spectroscopic Parameters, Electrode Potential, Acid Ionization Constants, and Alectron Exchange Rates of the ABTS Radicals and Ions, J. Phys. Chem. 97 (1993) 6710–6714. doi:10.1021/j100127a022.

[42] M. Vallet-Regí, F. Balas, M. Colilla, M. Manzano, Bone-regenerative bioceramic implants with drug and protein controlled delivery capability, Prog. Solid State Chem. 36 (2008) 163–191. doi:10.1016/j.progsolidstchem.2007.10.002.

[43] M. Piludu, L. Medda, F. Cugia, M. Monduzzi, A. Salis, Silver Enhancement for Transmission Electron Microscopy Imaging of Antibody Fragment–Gold Nanoparticles Conjugates Immobilized on Ordered Mesoporous Silica, Langmuir. 31 (2015) 9458–9463. doi:10.1021/acs.langmuir.5b02830.

[44] F. Cugia, S. Sedda, F. Pitzalis, D.F. Parsons, M. Monduzzi, A. Salis, Are specific buffer effects the new frontier of Hofmeister phenomena? Insights from lysozyme adsorption on ordered mesoporous silica, 6 (2016) 94617–94621. doi:10.1039/C6RA17356J.

[45] A. Salis, M.S. Bhattacharyya, M. Monduzzi, Specific ion effects on adsorption of lysozyme on functionalized SBA-15 mesoporous silica., J. Phys. Chem. B. 114 (2010) 7996–8001.

doi:10.1021/jp102427h.

[46] Aniket, D.A. Gaul, D.L. Bitterfield, J.T. Su, V.M. Li, I. Singh, et al., Enzyme dehydration using microglassification preserves the Protein's structure and function, J. Pharm. Sci. 104 (2015) 640–651. doi:10.1002/jps.24279.

[47] H. Yang, W. Wei, S. Liu, Monodispersed silica nanoparticles as carrier for co-immobilization of bi-enzyme and its application for glucose biosensing, Spectrochim. Acta - Part A Mol. Biomol. Spectrosc. 125 (2014) 183–188. doi:10.1016/j.saa.2014.01.004.

[48] H. Gustafsson, A. Küchler, K. Holmberg, P. Walde, Co-immobilization of enzymes with the help of a dendronized polymer and mesoporous silica nanoparticles, J. Mater. Chem. B. 3 (2015) 6174–6184. doi:10.1039/C5TB00543D.

[49] W. Chouyyok, J. Panpranot, C. Thanachayanant, S. Prichanont, Effects of pH and pore characters of mesoporous silicas on horseradish peroxidase immobilization, J. Mol. Catal. B Enzym. 56 (2009) 246–252. doi:10.1016/j.molcatb.2008.05.009.

**Figure caption**

**Scheme 1.** Flow diagram of the experimental work

**Scheme 2.** Cascade reactions catalyzed by GOx and HRP. A) The oxidation of glucose to gluconolactone leads to *in situ* $H_2O_2$ production. B) The latter is a substrate for HRP which oxidizes $ABTS^{2-}$ to $ABTS^{\bullet-}$.

**Fig.1** Physico-chemical characterization of SBA-15 and SBA-15-$NH_2$; A) TEM image (Bar, 100 nm); B) SAXS pattern of SBA-15 (large panel) and SBA-15-$NH_2$ (small panel); C) $N_2$ adsorption-desorption isotherms at 77K; D) pore size distribution calculated from the desorption branch; E) ATR-FTIR spectrum.

**Fig. 2** Co-immobilization kinetics of GOx and HRP on SBA-15 mesoporous silica. A) Decrease of protein concentration in the immobilizing solution; B) increase of protein loading (mg of protein per g of SBA-15) for different GOx:HRP mass ratios; C) fitting of kinetic data with a pseudo-second order model (eq. 3); D) fitting of kinetic data with an intraparticle diffusion model (eq. 4).

**Fig. 3** Enzymatic activity of HRP/GOx@SBA-15 dried biocatalyst at four different GOx:HRP mass ratios.

**Fig. 4** Biocatalyst stability: A) thermal stability; B) storage stability.

**Fig. 5** Biocatalyst recycling performance. Blue columns refer to the separately immobilized GOx@SBA-15/HRP@SBA-15 dry biocatalyst (GOx was covalently immobilized on SBA-15; HRP was physically immobilized at pH 8 on SBA-15); red columns refer to the same separately immobilized biocatalyst but where GOx@SBA-15 was dried, whereas HRP@SBA-15 was kept wet; green columns refer to the activity of the covalent co-immobilized GOx/HRP@SBA-15 which was kept wet.

**Fig. 6** Biocatalytic (wet GOx/HRP@SBA-15) oxidation of the recalcitrant phenolic compounds ferulic acid and caffeic acid. A) Concentration decrease and B) conversion of ferulic acid and caffeic acid as a function of reaction time.

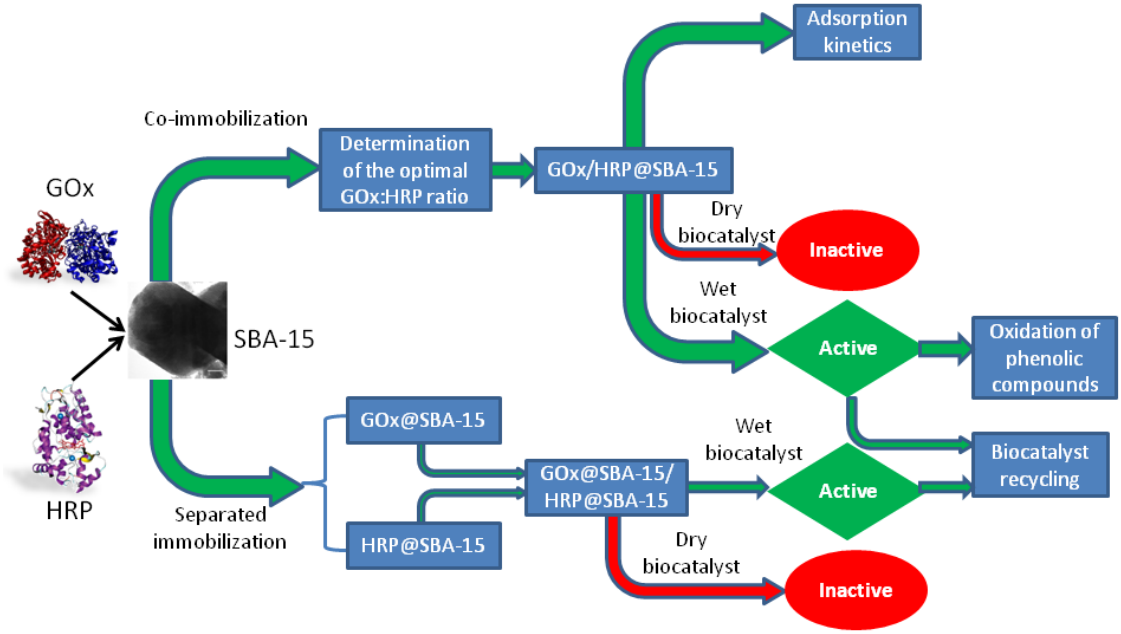
Adsorption kinetics
Co-immobilization
Determination of the optimal GOx:HRP ratio
GOx/HRP@SBA-15
GOx
Dry biocatalyst
Inactive
Wet biocatalyst
Active
Oxidation of phenolic compounds
SBA-15
GOx@SBA-15
Wet biocatalyst
Biocatalyst recycling
GOx@SBA-15/ HRP@SBA-15
Active
HRP
Separated immobilization
HRP@SBA-15
Dry biocatalyst
Inactive

**Scheme 1.**

**A)**

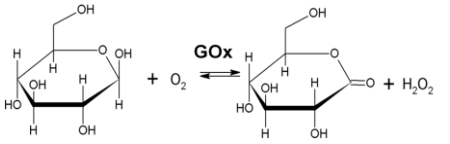


**B)**

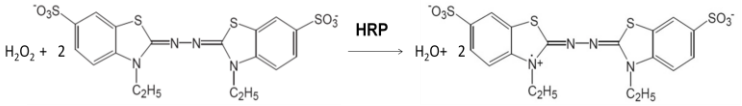


**Scheme 2.**

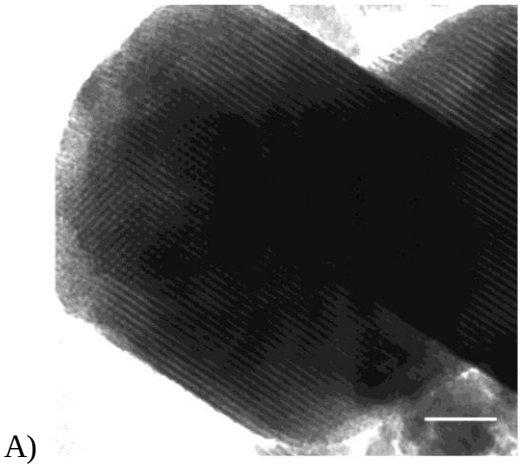

A)

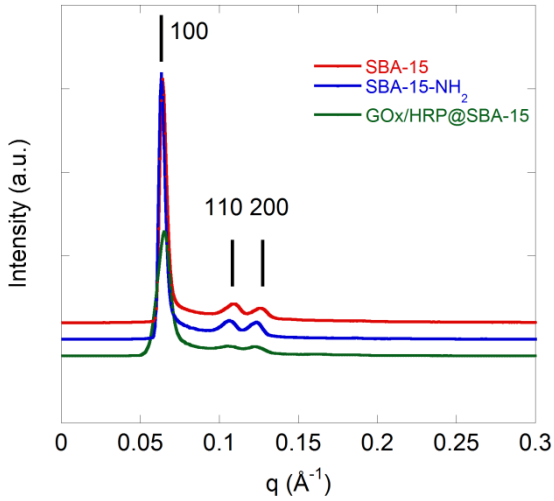
100
110 200
SBA-15
SBA-15-NH2
GOx/HRP@SBA-15
Intensity (a.u.)
0
0.05
0.1
0.15
0.2
0.25
0.3
q (Å-1)

B)

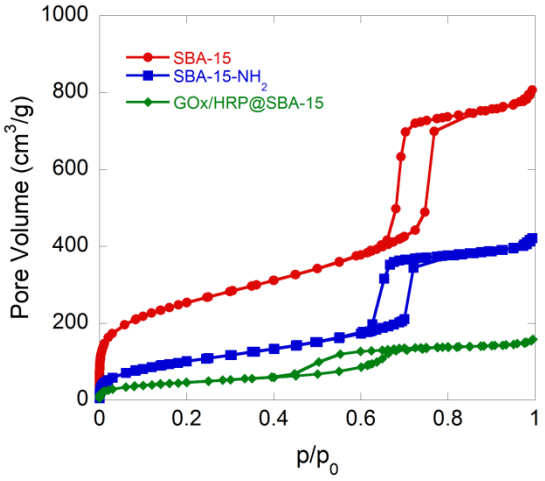
SBA-15
SBA-15-NH2
GOx/HRP@SBA-15
Pore Volume (cm3/g)
0
200
400
600
800
1000
0
0.2
0.4
0.6
0.8
1
p/p0

C)

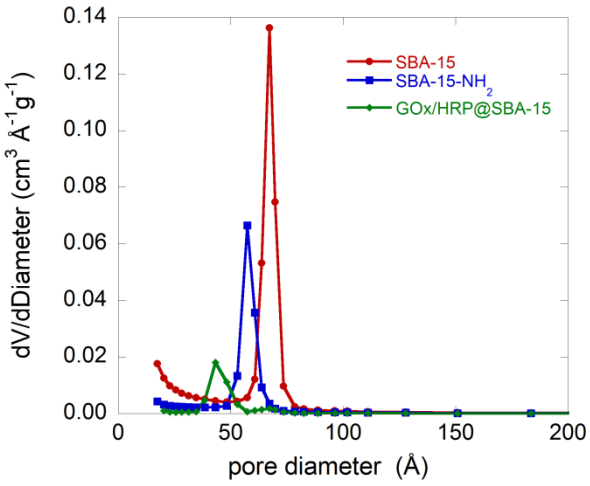
SBA-15
SBA-15-NH2
GOx/HRP@SBA-15
dV/dDiameter (cm3 Å-1g-1)
0.00
0.02
0.04
0.06
0.08
0.10
0.12
0.14
0
50
100
150
200
pore diameter (Å)

D)

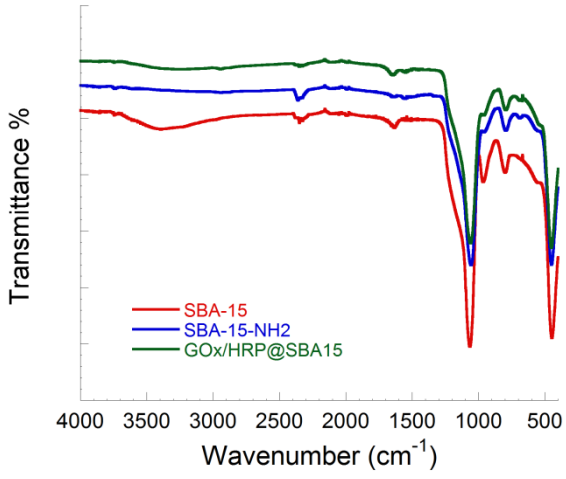
SBA-15
SBA-15-NH2
GOx/HRP@SBA15
Transmittance %
4000
3500
3000
2500
2000
1500
1000
500
Wavenumber (cm-1)

E)

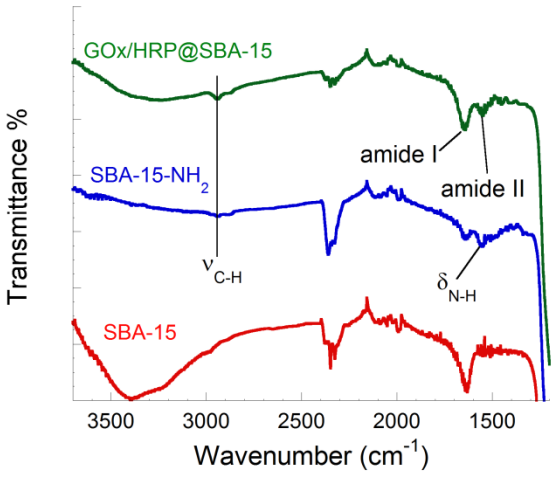
GOx/HRP@SBA-15
SBA-15-NH2
SBA-15
amide I
amide II
νC-H
δN-H
Transmittance %
3500
3000
2500
2000
1500
Wavenumber (cm-1)

F)

**Fig.1**

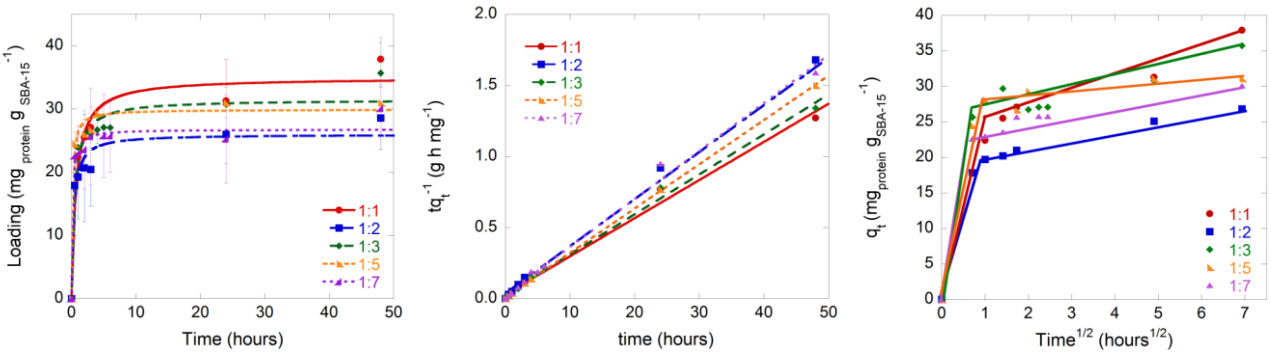
Loading (mg protein g SBA-15 -1)
Time (hours)
1:1
1:2
1:3
1:5
1:7
tqt-1 (g h mg-1)
time (hours)
qt (mgprotein gSBA-15 -1)
Time1/2 (hours1/2)

**Fig. 2**

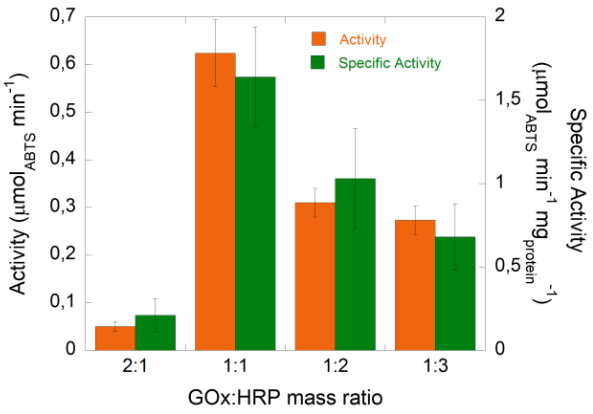
Activity
Specific Activity
Activity (µmol$_{ABTS}$ min$^{-1}$)
Specific Activity (µmol$_{ABTS}$ min$^{-1}$ mg$_{protein}$$^{-1}$)
0,7
0,6
0,5
0,4
0,3
0,2
0,1
0
2
1,5
1
0,5
0
2:1
1:1
1:2
1:3
GOx:HRP mass ratio

**Fig. 3**

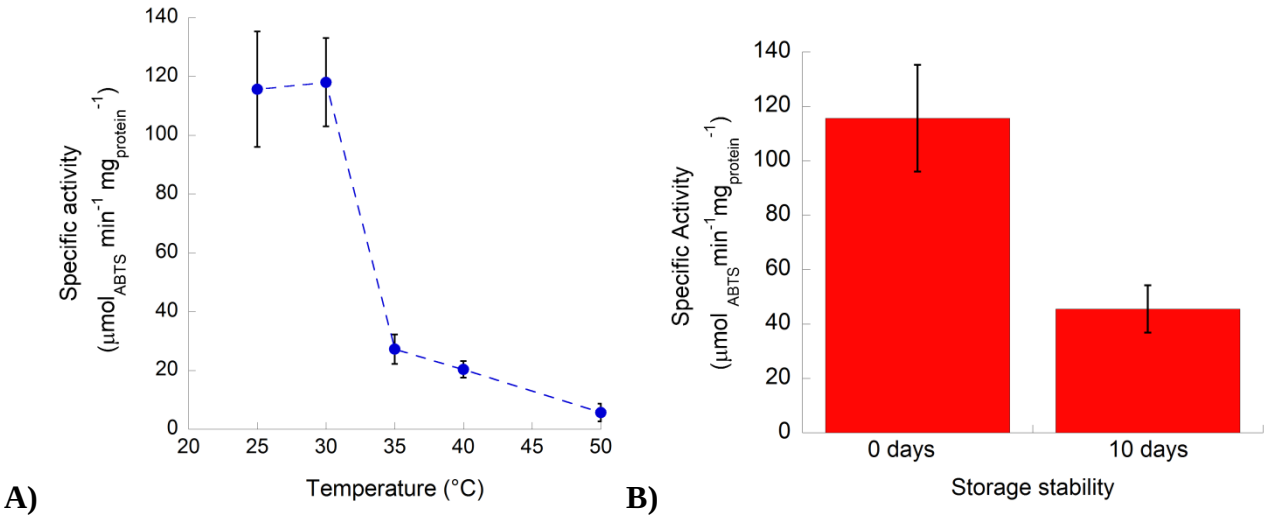


**Fig. 4.** Biocatalyst stability: A) thermal stability. B) storage stability.

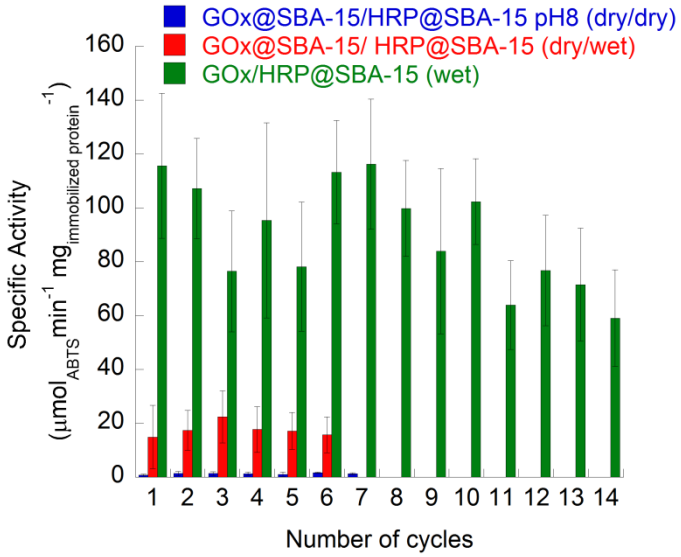
GOx@SBA-15/HRP@SBA-15 pH8 (dry/dry)
GOx@SBA-15/ HRP@SBA-15 (dry/wet)
GOx/HRP@SBA-15 (wet)
Specific Activity
(μmol$_{ABTS}$ min$^{-1}$ mg$_{immobilized\ protein}$$^{-1}$)
0
20
40
60
80
100
120
140
160
1 2 3 4 5 6 7 8 9 10 11 12 13 14
Number of cycles

**Fig. 5**

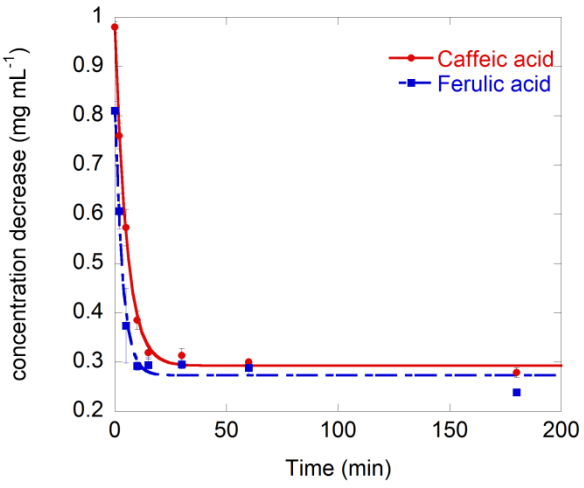
concentration decrease (mg mL-1)
Time (min)
Caffeic acid
Ferulic acid

A)

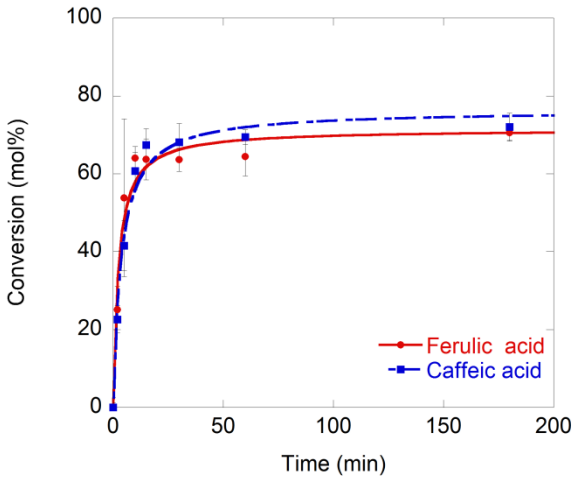
Conversion (mol%)
Time (min)
Ferulic acid
Caffeic acid

B)

**Fig. 6**